
Weighted finite difference methods for a nonlinear Klein–Gordon equation with high oscillations in space and time

Yanyan Shi¹, Christian Lubich¹

Abstract We consider a nonlinear Klein–Gordon equation in the nonrelativistic limit regime with initial data in the form of a modulated highly oscillatory exponential. In this regime of a small scaling parameter ε , the solution exhibits rapid oscillations in both time and space, posing challenges for numerical approximation. We propose an explicit and an implicit exponentially weighted finite difference method. While the explicit weighted leapfrog method needs to satisfy a CFL-type stability condition, the implicit weighted Crank–Nicolson method is unconditionally stable. Both methods achieve second-order accuracy with time steps and mesh sizes that are not restricted in magnitude by ε . The methods are uniformly convergent in the range from arbitrarily small to moderately bounded ε . Numerical experiments illustrate the theoretical results.

Keywords. Exponentially weighted finite difference method, nonlinear Klein–Gordon equation, highly oscillatory solution, dispersion relation, asymptotic-preserving, uniformly accurate.

Mathematics Subject Classification (2020): 65M06, 65M12, 65M15

1 Introduction

We consider the numerical solution of nonlinear dispersive wave equations that exhibit highly oscillatory behaviour in both time and space. As a concrete example, we focus on the nonlinear Klein–Gordon equation in the scaling known as the nonrelativistic limit regime; see e.g. [2, 1, 10, 5]. With a small parameter $0 < \varepsilon \ll 1$, we consider

$$\varepsilon^2 \partial_t^2 u - \partial_x^2 u + \frac{1}{\varepsilon^2} u + \lambda |u|^2 u = 0, \quad x \in \mathbb{R}, \quad 0 \leq t \leq T, \quad (1.1)$$

¹ Mathematisches Institut, Univ. Tübingen, D-72076 Tübingen, Germany.
E-mail: {Shi, Lubich}@na.uni-tuebingen.de

where the solution $u = u(t, x)$ is complex-valued. Here, λ is a fixed nonzero real number independent of ε , and T is a fixed final time. The initial conditions are given by modulated highly oscillatory exponentials,

$$u(0, x) = a_0(x)e^{i\kappa x/\varepsilon}, \quad \partial_t u(0, x) = \frac{1}{\varepsilon^2} b_0(x)e^{i\kappa x/\varepsilon}. \quad (1.2)$$

The initial conditions include a rapidly oscillating phase factor with a fixed wave number $\kappa \in \mathbb{R} \setminus \{0\}$. The functions $a_0, b_0 : \mathbb{R} \rightarrow \mathbb{C}$ are smooth profiles whose derivatives are uniformly bounded independently of ε and which have bounded support.

Our objective is to numerically approximate the solution over a fixed time interval $0 \leq t \leq T$ that is independent of ε . Numerically solving (1.1)–(1.2) is challenging due to the high oscillations of the solution in both time and space. The literature predominantly focuses on smooth initial data and handling temporal oscillations, with methods including finite difference schemes [2], splitting techniques [9], approaches based on Duhamel's formula [5], time-twoscale methods [6,3], and multiscale expansions [10,1]. However, only few numerical works address simultaneous spatial and temporal oscillations for (1.1) or related equations. We are aware of two approaches: the nonlinear geometric optics method of [8], where a wider class of partial differential equations with a wider class of highly oscillatory initial data than considered here is addressed using different numerical and analytical techniques, and the combination of analytical approximations with tailor-made time integration in [11] for a wider class of partial differential equations with highly oscillatory initial data that are real parts of (1.2).

In this work, we build on the approach in [15], where weighted finite difference methods for a nonlinear Schrödinger equation with highly oscillatory solutions in space and time were proposed and analyzed. These methods are conceptually simple and as easy to implement as classical finite difference methods. Here we study the nontrivial transfer and adaptation of the approach of [15] to the Klein–Gordon equation (1.1) with initial data (1.2). Introducing suitable weights into standard finite difference schemes enables us to use large time steps and mesh sizes that are not constrained by the small parameter ε . Our method employs co-moving coordinates, which allows us to maintain a relatively small spatial computational interval that is largely determined by the support of the initial conditions, while capturing the original solution across the entire domain. Furthermore, our approach can effectively resolve counter-propagating waves, as the solution exhibits two opposite time frequencies corresponding to distinct group velocities. The proposed method is not only asymptotic-preserving as $\varepsilon \rightarrow 0$ but also uniformly accurate for $0 < \varepsilon \leq 1$, recovering a standard co-moving finite difference scheme when the ratio of the time step and mesh size to ε approaches zero.

Section 2 presents an asymptotic analytical approximation of the continuous problem for small ε , which is of first order accuracy in ε for general initial data (1.2) and of second order for polarized initial data, for which the wave is uni-directional.

In Section 3, we describe the algorithm studied in this paper, which is applied to a reformulation of the initial-value problem (1.1)–(1.2) with co-moving coordinates. We introduce a weighted finite difference method that extends the classical explicit leapfrog method in time with central finite differences in space to the case of an arbitrarily small ε in (1.1)–(1.2). There is also an analogous extension of the implicit Crank–Nicolson method.

Section 4 states the main results of the paper and presents numerical experiments. We derive the leading term in the modulated Fourier expansion of the numerical solution and establish second order error bounds that allow time step sizes τ and mesh widths h to be chosen arbitrarily large compared to ε . For $h \gg \varepsilon$, the explicit method imposes a step-size restriction of the form $\tau \leq ch^2$, which is not required for the implicit method. For both methods we have $\mathcal{O}(h^2 + \tau^2 + \varepsilon)$ error bounds for general initial data (1.2), which improve to $\mathcal{O}(h^2 + \tau^2 + \varepsilon^2)$ for polarized initial data.

The results stated in Section 4 are proved in Sections 5 and 6. In Section 5, we analyze the consistency error, i.e., the defect arising when inserting a function with a controlled small distance to the exact solution into the numerical scheme. Section 6 presents a linear Fourier stability analysis, followed by a nonlinear stability analysis that bounds the numerical solution error in terms of the defect.

We add a remark on easy generalizations of the numerical methods and their analysis as studied here:

- First, the extension of the numerical methods and their error bounds to higher space dimensions in the Klein–Gordon equation is straightforward.
- While we consider the nonlinear Klein–Gordon equation with complex initial data (1.2), the numerical methods and theoretical results of this paper extend with minor modifications to the real case where the complex initial data in (1.2) are replaced by their real parts.
- Like in [15], the numerical methods and their theory can be extended to initial data that are sums of modulated exponentials with different wave numbers $\kappa_1, \dots, \kappa_m$. Such an extension is easily obtained when an $\mathcal{O}(h^2 + \tau^2 + \varepsilon)$ error bound is desired, but second order in ε would require a more substantial analytical and computational effort.

2 Preparation: Dominant terms and co-moving coordinates

Before introducing the numerical method, we give two approximation results for the solution of (1.1)–(1.2). We distinguish between general initial data (1.2) and polarized initial data, which yield an essentially uni-directional wave propagation. We further present a reformulation of the equation in co-moving coordinates, on which the numerical discretization will be based.

2.1 Solution approximation for general initial data

Up to an $\mathcal{O}(\varepsilon)$ error, the following result for oscillatory initial data (1.2) with wave number κ/ε yields bi-directional wave propagation having frequencies $\pm\omega/\varepsilon^2$ with $\omega = \sqrt{1 + \kappa^2}$ for the nonlinear Klein–Gordon equation (1.1) with oscillatory initial data (1.2), in accordance with the dispersion relation $\varepsilon^2(i\omega/\varepsilon^2)^2 - (i\kappa/\varepsilon)^2 + 1/\varepsilon^2 = 0$, i.e. $\omega^2 = \kappa^2 + 1$, of the linear Klein–Gordon equation. We often refer to κ and ω as the wave number and frequency instead of κ/ε and ω/ε^2 , respectively.

Proposition 2.1 (Dominant terms of the solution) *Let $u(t, x)$ be the solution of equation (1.1) for initial data (1.2) with $0 < \varepsilon \ll 1$, $\kappa \neq 0$ and smooth profile functions a_0 and b_0 . Then there exists c independent of ε such that*

$$\begin{aligned} \|u(t, \cdot) - \tilde{u}(t, \cdot)\|_{L^\infty} &\leq c\varepsilon, \quad 0 \leq t \leq T, \\ \varepsilon^2 \|\partial_t u(t, \cdot) - \partial_t \tilde{u}(t, \cdot)\|_{L^\infty} &\leq c\varepsilon, \quad 0 \leq t \leq T, \end{aligned}$$

where \tilde{u} has the form

$$\tilde{u}(t, x) = a^+(t, \xi)e^{i(\kappa x - \omega t/\varepsilon)/\varepsilon} + a^-(t, \eta)e^{i(\kappa x + \omega t/\varepsilon)/\varepsilon}, \quad (2.1)$$

with frequency $\omega = \sqrt{1 + \kappa^2}$, group velocity $c_g = \partial_\kappa \omega = \kappa/\omega < 1$, and with co-moving coordinates $\xi = x - c_g t/\varepsilon$, $\eta = x + c_g t/\varepsilon$. The functions $a^+(t, \xi)$ and $a^-(t, \eta)$ satisfy the following separated nonlinear Schrödinger equations:

$$\begin{aligned} 2i\omega \partial_t a^+ &= -(1 - c_g^2) \partial_\xi^2 a^+ + \lambda |a^+|^2 a^+, \\ a^+(0, \xi) &= \frac{1}{2}(a_0(\xi) + ib_0(\xi)/\omega), \\ -2i\omega \partial_t a^- &= -(1 - c_g^2) \partial_\eta^2 a^- + \lambda |a^-|^2 a^-, \\ a^-(0, \eta) &= \frac{1}{2}(a_0(\eta) - ib_0(\eta)/\omega). \end{aligned} \quad (2.2)$$

We observe that the equation for a^- is obtained by replacing ω by $-\omega$ and consequently $c_g = \kappa/\omega$ by $-c_g$ in the equation for a^+ . Note that the velocity behaves as $\partial_t u = \mathcal{O}(\varepsilon^{-2})$ so that the above error bound corresponds to the relative error.

The proof works in the functional setting of the Wiener algebra $A(\mathbb{R})$; see, e.g., [12] for properties of the Wiener algebra and [7] for its use in highly oscillatory nonlinear hyperbolic equations. The space $A(\mathbb{R})$ consists of all complex-valued functions $f : \mathbb{R} \rightarrow \mathbb{C}$ having a Fourier transform \hat{f} that is Lebesgue-integrable, i.e., $\hat{f} \in L^1(\mathbb{R})$. $A(\mathbb{R})$ is a Banach space with the norm

$$\|f\|_{A(\mathbb{R})} = \|\hat{f}\|_{L^1(\mathbb{R})} = \int_{\mathbb{R}} |\hat{f}(\theta)| d\theta.$$

The pointwise product of two functions $f, g \in A(\mathbb{R})$ is bounded by

$$\|fg\|_{A(\mathbb{R})} \leq \|f\|_{A(\mathbb{R})} \|g\|_{A(\mathbb{R})}, \quad (2.3)$$

which makes $A(\mathbb{R})$ a Banach algebra. The maximum norm of a function in $A(\mathbb{R})$ is bounded by its $A(\mathbb{R})$ -norm, and conversely, the $A(\mathbb{R})$ -norm is bounded by the maximum norm of the function and its derivative:

$$\|f\|_{L^\infty(\mathbb{R})} \leq \|f\|_{A(\mathbb{R})} \quad \text{and} \quad \|f\|_{A(\mathbb{R})} \leq c_1 \max(\|f\|_{L^\infty(\mathbb{R})}, \|f'\|_{L^\infty(\mathbb{R})}). \quad (2.4)$$

Proof Rather than directly estimating the error between u and \tilde{u} , we introduce a higher-order approximation as in [14]:

$$u_{\text{MFE}}(t, x) = (a^+ + \varepsilon b^+) e^{i(\kappa x - \omega t/\varepsilon)/\varepsilon} + (a^- + \varepsilon b^-) e^{i(\kappa x + \omega t/\varepsilon)/\varepsilon} - \frac{\varepsilon^2 \lambda}{\kappa^2 - 9\omega^2 + 1} \left((a^+)^2 \overline{a^-} e^{i(\kappa x - 3\omega t/\varepsilon)/\varepsilon} + \overline{a^+} (a^-)^2 e^{i(\kappa x + 3\omega t/\varepsilon)/\varepsilon} \right),$$

where $a^+ = a^+(t, \xi)$, $a^- = a^-(t, \eta)$ satisfy (2.2), and $b^+ = b^+(t, \xi^+, \xi^-)$, $b^- = b^-(t, \xi^+, \xi^-)$ satisfy the following equations

$$4i\kappa \partial_\eta b^+ = 2\lambda |a^-|^2 a^+, \quad 4i\kappa \partial_\xi b^- = 2\lambda |a^+|^2 a^-. \quad (2.5)$$

The defect obtained on inserting u_{MFE} into (1.1) is

$$d(t, x) = \varepsilon^2 \partial_t^2 u_{\text{MFE}} - \partial_x^2 u_{\text{MFE}} + \frac{1}{\varepsilon^2} u_{\text{MFE}} + \lambda |u_{\text{MFE}}|^2 u_{\text{MFE}}. \quad (2.6)$$

Using the expression of u_{MFE} , we have

$$\begin{aligned} d(t, x) = & \left(-2i\omega \partial_t a^+ - (1 - c_g^2) \partial_\xi^2 a^+ - 4i\kappa \partial_\eta b^+ \right. \\ & \left. + \lambda (|a^+|^2 a^+ + 2|a^-|^2 a^+) \right) e^{i(\kappa x - \omega t/\varepsilon)/\varepsilon} \\ & + \left(2i\omega \partial_t a^- - (1 - c_g^2) \partial_\eta^2 a^- - 4i\kappa \partial_\xi b^- \right. \\ & \left. + \lambda (|a^-|^2 a^- + 2|a^+|^2 a^-) \right) e^{i(\kappa x + \omega t/\varepsilon)/\varepsilon} \\ & + \left(\frac{(9\omega^2 - \kappa^2 - 1)\lambda}{\kappa^2 - 9\omega^2 + 1} + \lambda \right) (a^+)^2 \overline{a^-} e^{i(\kappa x - 3\omega t/\varepsilon)/\varepsilon} \\ & + \left(\frac{(9\omega^2 - \kappa^2 - 1)\lambda}{\kappa^2 - 9\omega^2 + 1} + \lambda \right) (a^-)^2 \overline{a^+} e^{i(\kappa x + 3\omega t/\varepsilon)/\varepsilon} + \mathcal{O}(\varepsilon). \end{aligned}$$

Since a^\pm and b^\pm satisfy equations (2.2) and (2.5), we obtain uniformly for $t \in [0, T]$

$$\|d(t, \cdot)\| = \mathcal{O}(\varepsilon),$$

where the norm can be the $BC(\mathbb{R})$ -norm (maximum norm of bounded continuous functions) or the stronger $BC^1(\mathbb{R})$ -norm (maximum norm of a bounded continuously differentiable function and its bounded derivative). The $BC^1(\mathbb{R})$ -norm is stronger than the norm of the Wiener algebra $A(\mathbb{R})$, as is implied by (2.4). Hence, the $\mathcal{O}(\varepsilon)$ defect bound is also valid in the $A(\mathbb{R})$ -norm. Comparing equation (2.6) with (1.1) shows that the error $e = u - u_{\text{MFE}}$ solves the evolution equation

$$\varepsilon^2 \partial_t^2 e - \partial_x^2 e + \frac{1}{\varepsilon^2} e + \lambda (|u|^2 u - |u_{\text{MFE}}|^2 u_{\text{MFE}}) + d = 0.$$

We rewrite this equation as a first-order system of the form and scaling as studied in a Wiener algebra setting in [7],

$$\partial_t \begin{pmatrix} e \\ s \\ z \end{pmatrix} = \frac{1}{\varepsilon} A(\partial_x) \begin{pmatrix} e \\ s \\ z \end{pmatrix} - \frac{1}{\varepsilon^2} E \begin{pmatrix} e \\ s \\ z \end{pmatrix} - \begin{pmatrix} 0 \\ \lambda(|u|^2 u - |u_{\text{MFE}}|^2 u_{\text{MFE}}) + d \\ 0 \end{pmatrix},$$

where $s = \varepsilon^2 \partial_t e$, $z = \varepsilon \partial_x e$ and

$$A(\partial_x) = \begin{pmatrix} 0 & 0 & 0 \\ 0 & 0 & \partial_x \\ 0 & \partial_x & 0 \end{pmatrix}, \quad E = \begin{pmatrix} 0 & -1 & 0 \\ 1 & 0 & 0 \\ 0 & 0 & 0 \end{pmatrix}.$$

The initial data $e(0)$, $s(0)$, and $z(0)$ are all of order ε . Using the arguments of [4, Lemma 5.2], which follows [7] in analyzing such systems using the Wiener algebra norm, then shows that $\|e(t)\|_{A(\mathbb{R})} = \mathcal{O}(\varepsilon)$ uniformly for $0 \leq t \leq T$, which yields the same bound in the weaker maximum norm. \square

Remark 2.1 Similar results can be found in [13, 14], where a different scaling is considered. Notably, using the Wiener algebra norm yields a sharper bound, improving the order of accuracy by 1/2 compared to the results in [14].

2.2 Solution approximation for polarized initial data

In the special case of polarized initial data (see [7, 4]), the solution essentially propagates in a single direction. To derive such initial data, we first rewrite equation (1.1) as a first-order system of the type studied in [7], with $A(\partial_x)$ and E as in the proof above,

$$\partial_t \begin{pmatrix} u \\ v \\ w \end{pmatrix} = \frac{1}{\varepsilon} A(\partial_x) \begin{pmatrix} u \\ v \\ w \end{pmatrix} - \frac{1}{\varepsilon^2} E \begin{pmatrix} u \\ v \\ w \end{pmatrix} - \begin{pmatrix} 0 \\ \lambda|u|^2 u \\ 0 \end{pmatrix}, \quad \begin{pmatrix} u(0, x) \\ v(0, x) \\ w(0, x) \end{pmatrix} = \begin{pmatrix} u_0(x) \\ v_0(x) \\ w_0(x) \end{pmatrix},$$

by introducing $v = \varepsilon^2 \partial_t u$ and $w = \varepsilon \partial_x u$. Consider the hermitian matrix

$$-A(\kappa) - iE = \begin{pmatrix} 0 & i & 0 \\ -i & 0 & -\kappa \\ 0 & -\kappa & 0 \end{pmatrix},$$

which has the three eigenvalues $0, \pm \sqrt{1 + \kappa^2}$. Let ω be one of the non-zero eigenvalues and $\nu = (1, -i\omega, i\kappa)^\top$ the corresponding eigenvector.

The initial data are called *polarized* if $(u_0(x), v_0(x), w_0(x))^\top$ is in the span of the eigenvector ν for all $x \in \mathbb{R}$. Corresponding to $u_0(x) = a_0(x)e^{i\kappa x/\varepsilon}$, we thus have the initial data

$$v_0(x) = -i\omega a_0(x)e^{i\kappa x/\varepsilon}, \quad w_0(x) = i\kappa a_0(x)e^{i\kappa x/\varepsilon}.$$

On the other hand, by definition of $u_0(x)$ we have

$$\varepsilon \partial_x u_0(x) = i\kappa a_0(x)e^{i\kappa x/\varepsilon} + \varepsilon \partial_x a_0(x)e^{i\kappa x/\varepsilon} \neq w_0(x) \quad \text{in general.}$$

To resolve this apparent contradiction and obtain initial data that are both polarized and fully consistent, we use the co-moving coordinate

$$\xi = x - c_g t / \varepsilon, \quad p(t, \xi) = u(t, x),$$

and consider the equation for the transformed variable p ,

$$\varepsilon^2 \partial_t^2 p - (1 - c_g^2) \partial_\xi^2 p - 2\varepsilon c_g \partial_t \partial_\xi p + \frac{1}{\varepsilon^2} p + \lambda |p|^2 p = 0, \quad p(0, \xi) = a(0, \xi) e^{i\kappa\xi/\varepsilon}.$$

This system is equivalent to the original equation. Importantly, we have the relation

$$\partial_t p(t, \xi) = \partial_t u(t, x) + \frac{c_g}{\varepsilon} \partial_x u(t, x).$$

Using the polarized initial data u_0, v_0, w_0 allows us to define

$$\varepsilon^2 \partial_t p(0, \xi) = v_0(\xi) + c_g w_0(\xi) = (-i\omega + i\kappa c_g) p(0, \xi), \quad (2.7)$$

and then recover a consistent initial time derivative for u by

$$\begin{aligned} \varepsilon^2 \partial_t u(0, x) &= \varepsilon^2 \partial_t p(0, x) - \varepsilon c_g \partial_x u_0(x) \\ &= v_0(x) + c_g (w_0(x) - \varepsilon \partial_x u_0(x)) \\ &= -i\omega a_0(x) e^{i\kappa x/\varepsilon} - \varepsilon c_g \partial_x a_0(x) e^{i\kappa x/\varepsilon}, \end{aligned}$$

where we use the above formula for $\partial_x u_0(x)$. We thus derive the initial data

$$u(0, x) = a_0(x) e^{i\kappa x/\varepsilon}, \quad \partial_t u(0, x) = -\frac{1}{\varepsilon^2} (i\omega a_0(x) + \varepsilon c_g \partial_x a_0(x)) e^{i\kappa x/\varepsilon}. \quad (2.8)$$

Proposition 2.2 (Dominant term in the case of polarized initial data)
Let $u(t, x)$ be the solution of equation (1.1) with polarized initial data (2.8). Then there exists a positive constant c such that

$$\begin{aligned} \|u(t, \cdot) - \tilde{u}(t, \cdot)\|_{L^\infty} &\leq c \varepsilon^2, \quad 0 \leq t \leq T, \\ \varepsilon^2 \|\partial_t u(t, \cdot) - \partial_t \tilde{u}(t, \cdot)\|_{L^\infty} &\leq c \varepsilon^2, \quad 0 \leq t \leq T, \end{aligned}$$

where \tilde{u} has the form

$$\tilde{u}(t, x) = (a(t, \xi) + \varepsilon b(t, \xi)) e^{i(\kappa x - \omega t/\varepsilon)/\varepsilon},$$

with $\xi = x - c_g t / \varepsilon$, frequency $\omega = \sqrt{1 + \kappa^2}$, and the group velocity $c_g = \partial_\kappa \omega = \kappa / \omega$. The functions $a(t, \xi)$ and $b(t, \xi)$ satisfy nonlinear and linear Schrödinger equations, respectively,

$$\begin{aligned} 2i\omega \partial_t a &= -(1 - c_g^2) \partial_\xi^2 a + \lambda |a|^2 a, \\ a(0, \xi) &= a_0(\xi) \\ 2i\omega \partial_t b &= -(1 - c_g^2) \partial_\xi^2 b + \lambda (2|a|^2 b + a^2 \bar{b}) - 2c_g \partial_t \partial_\xi a, \\ b(0, \xi) &= 0. \end{aligned} \quad (2.9)$$

Proof The defect obtained by inserting \tilde{u} into (1.1) is

$$d(t, x) = \varepsilon^2 \partial_t^2 \tilde{u} - \partial_x^2 \tilde{u} + \frac{1}{\varepsilon^2} \tilde{u} + \lambda |\tilde{u}|^2 \tilde{u}.$$

Using the expression of \tilde{u} , we compute

$$\begin{aligned} d(t, x) = & \underbrace{-(1 - c_g^2) \partial_\xi^2 a - 2i\omega \partial_t a + \lambda |a|^2 a}_{=0} \\ & - \varepsilon \underbrace{(2c_g \partial_t \partial_\xi a - (1 - c_g^2) \partial_\xi^2 b - 2i\omega \partial_t b + \lambda(2|a|^2 b + a^2 \bar{b}))}_{=0} + \mathcal{O}(\varepsilon^2), \end{aligned}$$

where we have used that all other terms cancel due to the equations for a and b . The remaining steps follow as in the proof of Proposition 2.1. \square

2.3 Reformulation in co-moving coordinates

By Proposition 2.1, the solution of (1.1) with initial data (1.2) admits the approximation

$$u(t, x) \approx \tilde{u}(t, x) = a^+(t, x - c_g t / \varepsilon) e^{i(\kappa x - \omega t / \varepsilon) / \varepsilon} + a^-(t, x + c_g t / \varepsilon) e^{i(\kappa x + \omega t / \varepsilon) / \varepsilon}.$$

This representation shows that the solution can be viewed as the superposition of two wave packets with the same wave number κ / ε , propagating in opposite directions with group velocity c_g / ε . Moreover, each wave packet evolves independently and can be obtained by solving the original equation (1.1) with appropriate polarized initial data, as characterized in Proposition 2.2. Consequently, we compute two approximate solutions of (1.1), each time with different polarized initial data corresponding to the two propagation directions, and then add the resulting solutions.

Since these wave packets travel over long distances on the real line in short time, working in a fixed spatial frame would require resolving rapid transport. Instead, we follow each wave packet in its natural moving frame, in which the solution remains spatially localized and evolves on an $\mathcal{O}(1)$ spatial scale, making the formulation more amenable to numerical discretization. To this end, we change to the co-moving coordinates

$$\xi = x - c_g t / \varepsilon, \quad \eta = x + c_g t / \varepsilon,$$

and obtain the following equations for functions $p(t, \xi)$ and $q(t, \xi)$ that are solutions to (1.1) in co-moving coordinates, equipped with polarized initial

data that correspond to the initial values of (2.2):

$$\begin{aligned} \varepsilon^2 \partial_t^2 p - (1 - c_g^2) \partial_\xi^2 p - 2\varepsilon c_g \partial_\xi \partial_t p + \frac{1}{\varepsilon^2} p + \lambda |p|^2 p = 0, \\ p(0, \xi) = a^+(0, \xi) e^{i\kappa\xi/\varepsilon}, \quad \partial_t p(0, \xi) = \frac{i\vartheta}{\varepsilon^2} p(0, \xi), \end{aligned} \quad (2.10)$$

$$\begin{aligned} \varepsilon^2 \partial_t^2 q - (1 - c_g^2) \partial_\eta^2 q + 2\varepsilon c_g \partial_t \partial_\eta q + \frac{1}{\varepsilon^2} q + \lambda |q|^2 q = 0, \\ q(0, \eta) = a^-(0, \eta) e^{i\kappa\eta/\varepsilon}, \quad \partial_t q(0, \eta) = \frac{-i\vartheta}{\varepsilon^2} q(0, \eta), \end{aligned} \quad (2.11)$$

where

$$\vartheta = \kappa c_g - \omega = -(1 - c_g^2) \omega = -1/\omega. \quad (2.12)$$

Since these equations have polarized initial data in the sense of (2.7), Proposition 2.2 shows that

$$\begin{aligned} p(t, \xi) = \tilde{p}(t, \xi) + \mathcal{O}(\varepsilon^2) \quad \text{with} \quad \tilde{p}(t, \xi) = a^+(t, \xi) e^{i\kappa\xi/\varepsilon} e^{i\vartheta t/\varepsilon^2}, \\ q(t, \eta) = \tilde{q}(t, \eta) + \mathcal{O}(\varepsilon^2) \quad \text{with} \quad \tilde{q}(t, \eta) = a^-(t, \eta) e^{i\kappa\eta/\varepsilon} e^{-i\vartheta t/\varepsilon^2}, \end{aligned} \quad (2.13)$$

where a^+ and a^- satisfy (2.2). Combining these estimates with Proposition 2.1, we conclude that

$$u(t, x) = p(t, \xi) + q(t, \eta) + \mathcal{O}(\varepsilon). \quad (2.14)$$

To sum up, we thus approximate the solution of the nonlinear Klein–Gordon equation (1.1) with (non-polarized) initial data (1.2) by the superposition of two solutions of (1.1) with polarized initial data that correspond to the two frequencies ω and $-\omega$. These two solutions are determined in co-moving coordinates as solutions of (2.10) and (2.11).

3 Weighted finite difference methods

In this section we derive and formulate the numerical methods that are proposed and analyzed in this paper.

3.1 Exponentially weighted finite differences

We proceed as in [15, Section 2]. For the second-order partial derivatives of $\tilde{p}(t, \xi) = a^+(t, \xi) e^{i\kappa\xi/\varepsilon} e^{i\vartheta t/\varepsilon^2}$, again with ϑ of (2.12), we note

$$\begin{aligned} \partial_t^2 \tilde{p}(t, \xi) &= \left(\left(\partial_t + \frac{i\vartheta}{\varepsilon^2} \right)^2 a^+(t, \xi) \right) e^{i\kappa\xi/\varepsilon} e^{i\vartheta t/\varepsilon^2}, \\ \partial_\xi^2 \tilde{p}(t, \xi) &= \left(\left(\partial_\xi + \frac{i\kappa}{\varepsilon} \right)^2 a^+(t, \xi) \right) e^{i\kappa\xi/\varepsilon} e^{i\vartheta t/\varepsilon^2}, \\ \partial_t \partial_\xi \tilde{p}(t, \xi) &= \left(\left(\partial_t + \frac{i\vartheta}{\varepsilon^2} \right) \left(\partial_\xi + \frac{i\kappa}{\varepsilon} \right) a^+(t, \xi) \right) e^{i\kappa\xi/\varepsilon} e^{i\vartheta t/\varepsilon^2}. \end{aligned}$$

We approximate the partial derivatives of a^+ by symmetric finite differences, with a temporal step size τ and a spatial grid size h , up to errors of $\mathcal{O}(\tau^2)$ and $\mathcal{O}(h^2)$ resulting from the Taylor expansion of the smooth function a^+ at (t, ξ) . We thus approximate, with $\alpha = \vartheta\tau/\varepsilon^2$,

$$\begin{aligned} \partial_t^2 \tilde{p}(t, \xi) &\approx \left(\frac{a^+(t + \tau, \xi) - 2a^+(t, \xi) + a^+(t - \tau, \xi)}{\tau^2} \right. \\ &\quad \left. + 2\frac{i\vartheta}{\varepsilon^2} \frac{a^+(t + \tau, \xi) - a^+(t - \tau, \xi)}{2\tau} - \frac{\vartheta^2}{\varepsilon^4} a^+(t, \xi) \right) e^{i\kappa\xi/\varepsilon} e^{i\vartheta t/\varepsilon^2} \\ &= \frac{e^{-i\alpha}(1 + i\alpha)\tilde{p}(t + \tau, \xi) - 2\tilde{p}(t, \xi) + e^{i\alpha}(1 - i\alpha)\tilde{p}(t - \tau, \xi)}{\tau^2} - \frac{\vartheta^2}{\varepsilon^4} \tilde{p}(t, \xi), \end{aligned}$$

and analogously for $\partial_\xi^2 p(t, \xi)$ and $\partial_t \partial_\xi p(t, \xi)$. Only the last term, which is dominant for small ε , is not a weighted finite difference.

3.2 Exponentially weighted leapfrog algorithm

We use weighted finite differences to discretize equations (2.10) and (2.11). We formulate the discretization of equation (2.10) for $p(t, \xi)$. The discretization of (2.11) for $q(t, \eta)$ is analogous, with the only modification that ω is replaced by $-\omega$.

Let $\tau > 0$ denote the time step and $h > 0$ the spatial mesh size. Using weighted finite differences, we obtain an explicit symmetric two-step scheme as follows:

$$\begin{aligned} &\varepsilon^2 \frac{e^{-i\alpha}(1 + i\alpha)p_j^{n+1} - 2p_j^n + e^{i\alpha}(1 - i\alpha)p_j^{n-1}}{\tau^2} \\ &- (1 - c_g^2) \frac{e^{-i\beta}(1 + i\beta)p_{j+1}^n - 2p_j^n + e^{i\beta}(1 - i\beta)p_{j-1}^n}{h^2} \\ &- 2\varepsilon c_g \left(\frac{e^{-i\alpha}(e^{-i\beta}p_{j+1}^{n+1} - e^{i\beta}p_{j-1}^{n+1}) - e^{i\alpha}(e^{-i\beta}p_{j+1}^{n-1} - e^{i\beta}p_{j-1}^{n-1})}{4\tau h} \right. \\ &\quad \left. + \frac{i\beta(e^{-i\alpha}p_j^{n+1} - e^{i\alpha}p_j^{n-1})}{2\tau h} + \frac{i\alpha(e^{-i\beta}p_{j+1}^n - e^{i\beta}p_{j-1}^n)}{2\tau h} \right) \\ &+ \lambda |p_j^n|^2 p_j^n = 0, \end{aligned} \quad (3.1)$$

where

$$\alpha = \frac{\vartheta\tau}{\varepsilon^2} = -(1 - c_g^2) \frac{\omega\tau}{\varepsilon^2} = -\frac{\tau}{\omega\varepsilon^2}, \quad \beta = \frac{\kappa h}{\varepsilon}, \quad (3.2)$$

and p_j^n approximates $p(t_n, \xi_j)$, where $t_n = n\tau$ and $\xi_j = jh$ for $n \in \mathbb{N}$ and $j \in \mathbb{Z}$.

Note that the terms in (3.1) correspond to those of (2.10). The dominant $\mathcal{O}(\varepsilon^{-2})$ terms that would appear in (3.1) cancel due to the dispersion relation $\omega^2 = 1 + \kappa^2$ together with $c_g = \kappa/\omega$ and $\vartheta = -1/\omega$: the factor multiplying p_j^n/ε^2 equals

$$-\vartheta^2 + (1 - c_g^2)\kappa^2 + 2c_g\vartheta\kappa + 1 = 0. \quad (3.3)$$

The velocity of $p(t, \xi)$ can be approximated by

$$\partial_t p(t_n, \xi_j) \approx \underbrace{\frac{e^{-i\alpha} p_j^{n+1} - e^{i\alpha} p_j^{n-1}}{2\tau}}_{=: \nu_j^n} + \frac{i\vartheta}{\varepsilon^2} p_j^n.$$

With the notation ν_j^n , scheme (3.1) can be rewritten in a compact form

$$\begin{aligned} & \varepsilon^2 \frac{e^{-i\alpha} p_j^{n+1} - 2p_j^n + e^{i\alpha} p_j^{n-1}}{\tau^2} - (1 - c_g^2) \frac{e^{-i\beta} p_{j+1}^n - 2p_j^n + e^{i\beta} p_{j-1}^n}{h^2} \\ & - 2\varepsilon c_g \frac{e^{-i\beta} \nu_{j+1}^n - e^{i\beta} \nu_{j-1}^n}{2h} - 2i\omega \nu_j^n + \lambda |p_j^n|^2 p_j^n = 0. \end{aligned}$$

As a starting step, we initialize the scheme with a weighted explicit Euler step

$$\begin{aligned} & \left(\frac{2\varepsilon^2}{\tau} - 2i\omega \right) \frac{e^{-i\alpha} p_j^0 - p_j^0}{\tau} - \frac{2\varepsilon^2}{\tau} \nu_j^0 - (1 - c_g^2) \frac{e^{-i\beta} p_{j+1}^0 - 2p_j^0 + e^{i\beta} p_{j-1}^0}{h^2} \\ & - 2\varepsilon c_g \frac{e^{-i\beta} \nu_{j+1}^0 - e^{i\beta} \nu_{j-1}^0}{2h} - 2i\omega \nu_j^0 + \lambda |p_j^0|^2 p_j^0 = 0, \\ & \text{with } p_j^0 = p(0, \xi_j), \quad \nu_j^0 = \partial_t p(0, \xi_j) - \frac{i\vartheta}{\varepsilon^2} p(0, \xi_j) = 0 \text{ by (2.10).} \end{aligned}$$

The weighted finite difference scheme tends to the classical leapfrog scheme in the limit $\tau/\varepsilon^2 \rightarrow 0$ and $h/\varepsilon \rightarrow 0$. Our main interest here is, however, to use the weighted scheme with large ratios τ/ε^2 and h/ε .

For this explicit method, we need a CFL-type stability condition:

$$\begin{aligned} 2\kappa^2 |\alpha| & \leq \beta^2 \quad \text{for } |\beta| \geq 1, \\ |\kappa| |\alpha| & \leq |\beta| \quad \text{for } |\beta| < 1. \end{aligned} \tag{3.4}$$

This requires that $\tau \leq \max(c_1 h^2, c_2 \varepsilon h)$, where c_1 and c_2 depend only on κ .

In practice, the sequence $(p_j^n)_{j \in \mathbb{Z}}$ must be truncated to a finite-dimensional vector, typically by imposing periodic boundary conditions over a finite interval. In this paper we will not study the error due to the truncation to a finite interval.

Having obtained p_j^n and q_j^n from the proposed scheme, we compute the velocities as

$$\begin{aligned} \varepsilon^2 v_{+,j}^n &= -i\omega p_j^n - \varepsilon c_g \frac{e^{-i\beta} p_{j+1}^n - e^{i\beta} p_{j-1}^n}{2h} + \varepsilon^2 \frac{e^{-i\alpha} p_j^{n+1} - e^{i\alpha} p_j^{n-1}}{2\tau} \quad (3.5) \\ \varepsilon^2 v_{-,j}^n &= i\omega q_j^n + \varepsilon c_g \frac{e^{-i\beta} q_{j+1}^n - e^{i\beta} q_{j-1}^n}{2h} + \varepsilon^2 \frac{e^{i\alpha} q_j^{n+1} - e^{-i\alpha} q_j^{n-1}}{2\tau}. \end{aligned}$$

Then we can construct approximations of the solution u and its time derivative $\partial_t u$ as follows.

Algorithm 3.1 (Reconstruction of u and $\partial_t u$ from p and q) We construct an approximation of the solution $u(t, x)$ to (1.1) by distinguishing two cases:

1. *Well-separated wave packets:* When the wave packets are spatially separated, the solution is obtained by directly combining the two components. With $s^n = c_g t_n / \varepsilon$,

$$\begin{aligned} u^n(\xi_j + s^n) &= p_j^n, & u^n(\eta_j - s^n) &= q_j^n, \\ v^n(\xi_j + s^n) &= v_{+,j}^n, & v^n(\eta_j - s^n) &= v_{-,j}^n \end{aligned}$$

2. *Overlapping wave packets:* When the wave packets overlap, the solution is constructed using interpolation:

$$\begin{aligned} u_i^n &= \mathcal{I}(\{p_j^n\}, x_i) + \mathcal{I}(\{q_j^n\}, x_i), \\ v_i^n &= \mathcal{I}(\{v_{+,j}^n\}, x_i) + \mathcal{I}(\{v_{-,j}^n\}, x_i), \end{aligned}$$

where x_i denotes the global grid points, and \mathcal{I} is an interpolation operator ensuring a smooth transition in the overlapping region. In practice, this is implemented by interpolating the envelope values $a_j^{\pm,n}$ onto the global grid, with a piecewise linear or quadratic interpolation, followed by reconstruction via (2.13)–(2.14).

With localized wave packets, the well-separated case occurs after a short time interval of length $\mathcal{O}(\varepsilon)$ in view of the two opposed group velocities $\pm c_g / \varepsilon$, so that interpolation is only rarely required for small ε , and not at all when $\tau \gg \varepsilon$.

3.3 Exponentially weighted Crank–Nicolson algorithm

Using the same approach, we derive the following weighted Crank–Nicolson type scheme:

$$\begin{aligned} & \varepsilon^2 \frac{e^{-i\alpha}(1 + i\alpha)p_j^{n+1} - 2p_j^n + e^{i\alpha}(1 - i\alpha)p_j^{n-1}}{\tau^2} \\ & - (1 - c_g^2) \frac{e^{-i\beta}(1 + i\beta)\check{p}_{j+1}^n - 2\check{p}_j^n + e^{i\beta}(1 - i\beta)\check{p}_{j-1}^n}{h^2} \\ & - 2\varepsilon c_g \left(\frac{e^{-i\alpha}(e^{-i\beta}p_{j+1}^{n+1} - e^{i\beta}p_{j-1}^{n+1}) - e^{i\alpha}(e^{-i\beta}p_{j+1}^{n-1} - e^{i\beta}p_{j-1}^{n-1})}{4\tau h} \right. \\ & \quad \left. + \frac{i\beta(e^{-i\alpha}p_j^{n+1} - e^{i\alpha}p_j^{n-1})}{2\tau h} + \frac{i\alpha(e^{-i\beta}\check{p}_{j+1}^n - e^{i\beta}\check{p}_{j-1}^n)}{2\tau h} \right) \\ & + \lambda \frac{(|p_j^{n+1}|^2 + |p_j^{n-1}|^2)\check{p}_j^n}{2} = 0, \end{aligned} \tag{3.6}$$

with $\check{p}_j^n = \frac{1}{2}(e^{-i\alpha}p_j^{n+1} + e^{i\alpha}p_j^{n-1})$. This implicit method is unconditionally stable.

4 Main results and numerical experiments

4.1 Results for general initial data

The following result provides the dominant term of the modulated Fourier expansion of the numerical solution to (3.1). Here we recall that ϑ is defined by (2.12).

Theorem 4.1 (Dominant terms of the numerical solution) *Let p_j^n and q_j^n be the numerical solution obtained using the explicit weighted leapfrog finite difference algorithm (3.1), under the stability condition (3.4). Assume that the solutions $a^\pm(t, \xi)$ of the nonlinear Schrödinger equation (2.2) have sufficiently many bounded partial derivatives. Then p_j^n and q_j^n can be written as*

$$\begin{aligned} p_j^n &= a^+(t, \xi) e^{i\kappa\xi/\varepsilon} e^{i\vartheta t/\varepsilon^2} + R^+(t, \xi), \\ q_j^n &= a^-(t, \xi) e^{i\kappa\xi/\varepsilon} e^{-i\vartheta t/\varepsilon^2} + R^-(t, \xi), \end{aligned}$$

for $t = n\tau$ and $\xi = jh$, where $a^\pm(t, \xi)$ satisfy (2.2), and the remainder term is bounded by

$$\|R^\pm\|_{L^\infty([0, T] \times \mathbb{R})} \leq C(\tau^2 + h^2 + \varepsilon).$$

Here, C is independent of ε, τ, h , but depends on the final time T .

The same error bound holds true for the implicit weighted Crank–Nicolson finite difference method (3.6) without any stability condition between τ and h .

A further main result of this paper is the following error bound for the weighted finite difference method. It follows directly from Algorithm 3.1, the modulated Fourier expansion of the exact solution in Proposition 2.1 and the modulated Fourier expansion of the numerical solution in Theorem 4.1. Note that the velocity behaves as $\partial_t u = \mathcal{O}(\varepsilon^{-2})$ so that the error bound given below corresponds to the relative error.

Theorem 4.2 (Error bound) *Under the assumptions of Theorem 4.1, we obtain the error bounds*

$$\begin{aligned} |u^n(x_i) - u(t_n, x_i)| &= \mathcal{O}(\tau^2 + h^2 + \varepsilon), \\ \varepsilon^2 |v^n(x_i) - \partial_t u(t_n, x_i)| &= \mathcal{O}(\tau^2 + h^2 + \varepsilon), \end{aligned}$$

uniformly for $t_n = n\tau \leq T$ and x_i . The constant symbolized by the \mathcal{O} -notation is independent of ε , the time step τ , and the mesh size h , but depends on the final time T .

The same error bounds hold true for the implicit weighted Crank–Nicolson finite difference method (3.6) without any stability condition between τ and h .

In the less interesting regime where $\tau \ll \varepsilon^2$ and $h \ll \varepsilon$, the method can be applied directly to approximate the original equation by solving only $p(t, \xi)$

or $q(t, \eta)$. For instance, one can set $q \equiv 0$ (or, alternatively, $p \equiv 0$) with initial data

$$\begin{aligned} p(0, \xi) &= u(0, \xi), & \partial_t p(0, \xi) &= \partial_t u(0, \xi) + \frac{c_g}{\varepsilon} \partial_x u(0, \xi), \\ q(0, \eta) &= 0, & \partial_t q(0, \eta) &= 0. \end{aligned} \quad (4.1)$$

To implement, it suffices to include a conditional check in the code of setting the initial data for p and q as follows:

If $h^2 \geq c\varepsilon^5$, then we set p^0 and q^0 according to the initial data (2.10)–(2.11).

Else we set p^0 and q^0 as (4.1).

Remark 4.1 A standard Taylor expansion yields an error bound of $\mathcal{O}(\tau^2/\varepsilon^6 + h^2/\varepsilon^4)$. Consequently, the error satisfies

$$|u^n(x_i) - u(t_n, x_i)| \leq \min \left(C_0(\tau^2 + h^2 + \varepsilon), C_1 \left(\frac{\tau^2}{\varepsilon^6} + \frac{h^2}{\varepsilon^4} \right) \right),$$

uniformly for t_n , x_i , and $0 < \varepsilon \leq 1$. Maximizing this bound over $0 < \varepsilon \leq 1$ gives the optimal balance $\varepsilon^7 \sim \tau^2$, $\varepsilon^5 \sim h^2$, leading to a uniform accuracy of $\mathcal{O}(\tau^{2/7} + h^{2/5})$ in the maximum norm for all $0 < \varepsilon \leq 1$. The optimal quadratic convergence rate is achieved when $\varepsilon \sim 1$ or $\varepsilon \leq \tau^2 + h^2$.

4.2 Polarized initial data

In this case, the solution propagates in a single direction and it suffices to solve only one of the equations for either $p(t, \xi)$ or $q(t, \eta)$. This also allows for an improved error bound.

The following theorem states the error bound for the case $\omega = \sqrt{1 + \kappa^2}$, i.e., when $u(t, x) = p(t, \xi)$ with p satisfying (2.10). The case $\omega = -\sqrt{1 + \kappa^2}$ is analogous, with q replacing p .

Theorem 4.3 (Error bound for polarized initial data) *Let p_j^n denote the numerical solution obtained from the weighted finite difference algorithm (3.1), under the stability condition (3.4). Assume polarized initial data with a single frequency ω associated with κ , and let the assumptions of Theorem 4.1 hold. Then there are the error bounds (with $x_j^n = \xi_j + c_g t_n / \varepsilon$)*

$$\begin{aligned} |p_j^n - u(t_n, x_j^n)| &= \mathcal{O}(\tau^2 + h^2 + \varepsilon^2), \\ \varepsilon^2 |v_{+,j}^n - \partial_t u(t_n, x_j^n)| &= \mathcal{O}(\tau^2 + h^2 + \varepsilon^2), \end{aligned}$$

for $t_n = n\tau \leq T$, $\xi_j = jh$. Here, the constant symbolized by the \mathcal{O} -notation is independent of τ , h , and $0 < \varepsilon \leq 1$, but depends on the final time T and the coefficient appearing in the stability condition (3.4).

The same error bounds hold true for the implicit weighted Crank-Nicolson finite difference method (3.6) without any stability condition between τ and h .

4.3 Numerical experiments

We consider the one-dimensional nonlinear Klein–Gordon equation (1.1) with $\lambda = 1$. The final time is set to $T = 0.5$. Numerical errors are measured at T in the discrete maximum norm.

Instead of solving the equation on the whole real line, we compute the transformed variables $p(t, \xi)$ and $q(t, \eta)$ on the bounded interval $\xi, \eta \in [-L, L]$ with $L = 8$, which is large enough to fully contain the localized wave packets and allow the use of periodic boundary conditions.

To implement Algorithm 3.1, we distinguish two cases based on the condition

$$L - c_g t / \varepsilon \leq -L + c_g t / \varepsilon, \quad \text{i.e., } c_g t \geq L \varepsilon.$$

If this condition is satisfied, the two wave packets, which move with group velocities $\pm c_g / \varepsilon$, are separated at time t . Otherwise, the wave packets overlap and interpolation is required, as described in the algorithm. For polarized initial data, there is only one wave packet and no such distinction is needed.

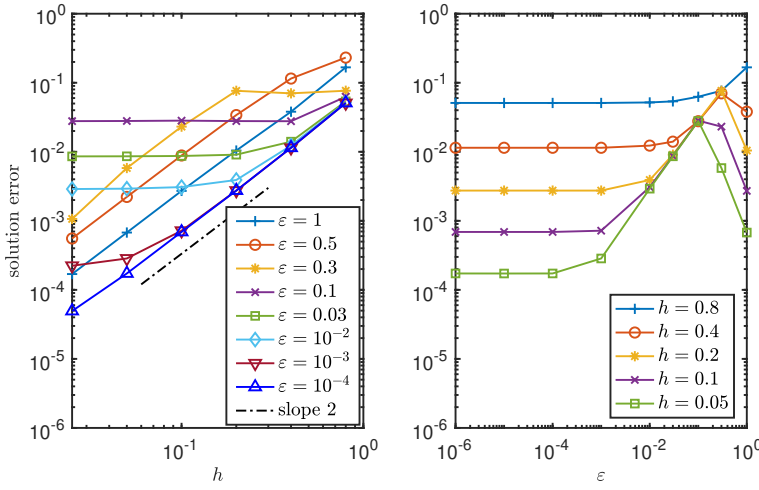


Fig. 4.1 General highly oscillatory initial data (1.2). Left: error vs. h for different values of ε . Right: error vs. ε for different values of h . The time step is chosen according to (4.2).

We first test our method for non-polarized initial data

$$u(0, x) = e^{-x^2} e^{ix/\varepsilon}, \quad \partial_t u(0, x) = \frac{1}{\varepsilon^2} e^{-x^2} e^{ix/\varepsilon}.$$

The left panel of Figure 4.1 shows the relative error in u plotted against h for several fixed values of ε . We observe that the error initially scales as h^2 and reaches a level of $\mathcal{O}(\varepsilon)$, in agreement with the asymptotic estimate in Theorem 4.2. Once h becomes sufficiently small such that $h^2 \leq c\varepsilon^5$ (with

$c = 5$ in this test), the error resumes its h^2 behavior. The right panel shows the error plotted against ε for several fixed values of h . For small ε , the error levels off at a value proportional to h^2 . We chose the time step size

$$\tau = \max(h^2/4, \varepsilon h/10) \quad (4.2)$$

so that the stability condition (3.4) is satisfied for all h and ε . With this choice, τ scales like h^2 for small ε , while a linear dependence on h is sufficient for larger ε .

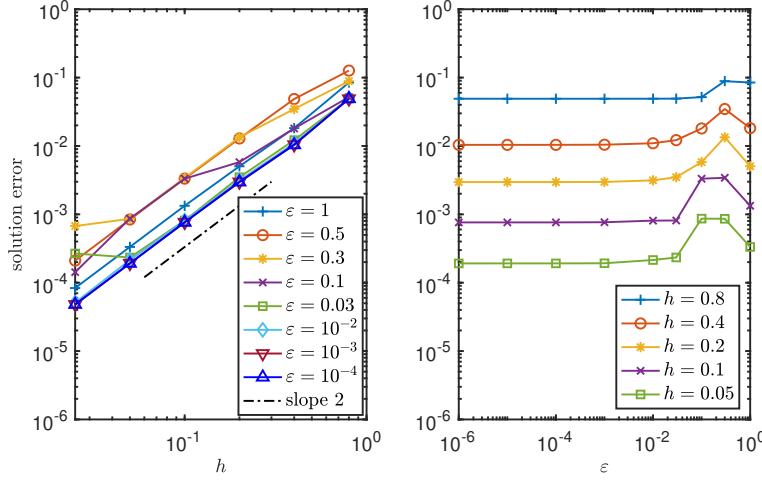


Fig. 4.2 Polarized initial data. Left: error vs. h for different values of ε . Right: error vs. ε for different values of h . The time step is chosen according to (4.2).

Next, we consider polarized initial data (2.8)

$$u(0, x) = e^{-x^2} e^{ix/\varepsilon}, \quad \partial_t u(0, x) = \left(-\frac{i\omega}{\varepsilon^2} + \frac{2c_g x}{\varepsilon} \right) e^{-x^2} e^{ix/\varepsilon}.$$

For this case, the frequency is $\omega = \sqrt{2}$ and the group velocity is $c_g = 1/\sqrt{2}$. The left panel of Figure 4.2 shows the relative error in p versus h for several fixed values of ε , while the right panel shows the error plotted against ε . Compared to the non-polarized case, the error is reduced for intermediate values of ε , which is consistent with Theorem 4.3, where the accuracy in ε improves from $\mathcal{O}(\varepsilon)$ to $\mathcal{O}(\varepsilon^2)$ for polarized initial data.

For the velocity error, we observe similar behavior. Moreover, comparable results are obtained for the weighted Crank–Nicolson method, and are therefore omitted for brevity.

5 Consistency

With the solution $a^+(t, \xi)$ of the first nonlinear Schrödinger initial value problem in (2.2), we consider the defect obtained on inserting

$$\tilde{p}(t, \xi) = a^+(t, \xi) e^{i\kappa\xi/\varepsilon} e^{i\vartheta t/\varepsilon^2}$$

into the weighted finite difference scheme (3.1),

$$\begin{aligned} d(t, \xi) := & \varepsilon^2 \frac{e^{-i\alpha}(1 + i\alpha)\tilde{p}(t + \tau, \xi) - 2\tilde{p}(t, \xi) + e^{i\alpha}(1 - i\alpha)\tilde{p}(t - \tau, \xi)}{\tau^2} \\ & - (1 - c_g^2) \frac{e^{-i\beta}\tilde{p}(t, \xi + h) - 2\tilde{p}(t, \xi) + e^{i\beta}\tilde{p}(t, \xi - h)}{h^2} \\ & - 2\varepsilon c_g \left(\frac{e^{-i\alpha}(e^{-i\beta}\tilde{p}(t + \tau, \xi + h) - e^{i\beta}\tilde{p}(t + \tau, \xi - h))}{4\tau h} \right. \\ & \quad \left. - \frac{e^{i\alpha}(e^{-i\beta}\tilde{p}(t - \tau, \xi + h) - e^{i\beta}\tilde{p}(t - \tau, \xi - h))}{4\tau h} \right. \\ & \quad \left. + \frac{i\beta(e^{-i\alpha}\tilde{p}(t + \tau, \xi) - e^{i\alpha}\tilde{p}(t - \tau, \xi))}{2\tau h} \right) \\ & + \lambda |\tilde{p}(t, \xi)|^2 \tilde{p}(t, \xi), \end{aligned} \quad (5.1)$$

where the two terms arising from the spatial discretization in (3.1) cancel by using the relation $(1 - c_g^2)i\beta/h + \varepsilon c_g i\alpha/\tau = 0$.

5.1 Defect bound in the maximum norm

Lemma 5.1 *In the situation of Theorem 4.1, the defect (5.1) is bounded in the maximum norm by*

$$\|d\|_{L^\infty([0, T] \times \mathbb{R})} \leq c(\tau^2 + h^2 + \varepsilon),$$

where c is independent of ε , τ , h and n with $t_n = n\tau \leq T$.

Proof The $\mathcal{O}(\tau^2)$ and $\mathcal{O}(h^2)$ error bounds of the weighted finite differences in Section 3.1 yield, omitting the omnipresent argument (t, ξ) on the right-hand side,

$$\begin{aligned} d(t, \xi) &= \left(\varepsilon^2 \partial_t^2 \tilde{p} - (1 - c_g^2) \partial_\xi^2 \tilde{p} - 2\varepsilon c_g \partial_t \partial_\xi \tilde{p} + \frac{\tilde{p}}{\varepsilon^2} + \lambda |\tilde{p}|^2 \tilde{p} \right) \\ &\quad - \underbrace{\left(-\vartheta^2 + (1 - c_g^2)\kappa^2 + 2c_g \vartheta \kappa + 1 \right)}_{=0 \text{ by the dispersion relation, see (3.3)}} \frac{\tilde{p}}{\varepsilon^2} + \mathcal{O}(\tau^2 + h^2) \\ &= \underbrace{\left(-2i\omega \partial_t a^+ - (1 - c_g^2) \partial_\xi^2 a^+ + \lambda |a^+|^2 a^+ \right)}_{=0 \text{ by (2.2)}} e^{i\kappa\xi/\varepsilon} e^{i\vartheta t/\varepsilon^2} \\ &\quad + \mathcal{O}(\tau^2 + h^2 + \varepsilon). \end{aligned}$$

This yields the stated result. \square

Remark 5.1 For polarized initial data, the defect is in fact smaller:

$$\|d\|_{L^\infty([0,T]\times\mathbb{R})} = \mathcal{O}(\tau^2 + h^2 + \varepsilon^2),$$

where d is defined in (5.1), but now with

$$\tilde{p}(t, \xi) = (a(t, \xi) + \varepsilon b(t, \xi)) e^{i\kappa\xi/\varepsilon} e^{i\vartheta t/\varepsilon^2},$$

and where $a(t, \xi)$ and $b(t, \xi)$ are the solutions of (2.9).

5.2 Defect bound in the Wiener algebra norm

The maximum norm in the defect bound of Lemma 5.1 turns out to be too weak a norm for the proof of Theorems 4.1 and 4.2. We need a defect bound in the norm of the Wiener algebra $A(\mathbb{R})$; see the summary in Section 2.1. The space $C([0, T], A(\mathbb{R}))$ in the following lemma is the Banach space of $A(\mathbb{R})$ -valued continuous functions on the interval $[0, T]$, with $\|d\|_{C([0, T], A(\mathbb{R}))} = \max_{0 \leq t \leq T} \|d(t, \cdot)\|_{A(\mathbb{R})}$.

Lemma 5.2 *In the situation of Theorem 4.1, the defect (5.1) is bounded in the Wiener algebra norm by*

$$\|d\|_{C([0, T], A(\mathbb{R}))} \leq c(\tau^2 + h^2 + \varepsilon),$$

where c is independent of ε , τ , h , and n with $t_n = n\tau \leq T$.

Proof The proof is based on (2.4) and follows the same steps as the proof in [15, Lemma 4.2]. \square

The same defect bound (possibly with a different constant c) is obtained for the weighted Crank–Nicolson method, using the same arguments.

6 Stability

6.1 Linear stability analysis in the Wiener algebra

In this subsection we give linear stability results for the weighted finite difference scheme. We bound the numerical solution corresponding to the linear Klein–Gordon equation (1.1) (without the nonlinearity) in the Wiener algebra norm, using Fourier analysis.

We momentarily omit the nonlinearity and interpolate the weighted finite difference scheme (3.1) from discrete spatial points $\xi_j = jh$, $j \in \mathbb{Z}$, to arbitrary

$\xi \in \mathbb{R}$ by setting

$$\begin{aligned} & \varepsilon^2 \frac{e^{-i\alpha}(1+i\alpha)p^{n+1}(\xi) - 2p^n(\xi) + e^{i\alpha}(1-i\alpha)p^{n-1}(\xi)}{\tau^2} \\ & + (c_g^2 - 1) \frac{e^{-i\beta}p^n(\xi + h) - 2p^n(\xi) + e^{i\beta}p^n(\xi - h)}{h^2} \\ & - 2\varepsilon c_g \left(\frac{e^{-i\alpha}(e^{-i\beta}p^{n+1}(\xi + h) - e^{i\beta}p^{n+1}(\xi - h))}{4\tau h} \right. \\ & \quad \left. - \frac{e^{i\alpha}(e^{-i\beta}p^{n-1}(\xi + h) - e^{i\beta}p^{n-1}(\xi - h))}{4\tau h} \right. \\ & \quad \left. + \frac{i\beta(e^{-i\alpha}p^{n+1}(\xi) - e^{i\alpha}p^{n-1}(\xi))}{2\tau h} \right) = 0. \end{aligned} \quad (6.1)$$

We clearly have $p^n(\xi_j) = p_j^n$ of (3.1) for all $n \geq 2$ if this holds true for $n = 0$ and $n = 1$. In particular, we have $\max_j |p_j^n| \leq \max_{\xi \in \mathbb{R}} |p^n(\xi)| \leq \|p^n\|_{A(\mathbb{R})}$.

Lemma 6.1 (Linear stability of the weighted leapfrog method) *Under condition (3.4), the weighted finite difference algorithm (6.1) without the nonlinear term is stable: There exists a norm $\|\cdot\|$ on $A(\mathbb{R}) \times A(\mathbb{R})$, equivalent to the norm $\|\cdot\|_{A(\mathbb{R}) \times A(\mathbb{R})}$ uniformly in ε, τ, h subject to (3.4), such that*

$$\|P^n\| = \|P^{n-1}\|, \quad \text{where } P^n = \begin{pmatrix} p^{n+1} \\ p^n \end{pmatrix}.$$

Proof Let $\hat{p}^n(\theta)$ be the Fourier transform of $p^n(\xi)$, i.e.,

$$p^n(\xi) = \frac{1}{2\pi} \int_{\mathbb{R}} \hat{p}^n(\theta) e^{i\theta\xi} d\theta.$$

Substituting this into (6.1) yields, for all ξ ,

$$\begin{aligned} & \frac{1}{2\pi} \int_{\mathbb{R}} e^{i\theta\xi} \left(\varepsilon^2 \frac{e^{-i\alpha}(1+i\alpha)\hat{p}^{n+1}(\theta) - 2\hat{p}^n(\theta) + e^{i\alpha}(1-i\alpha)\hat{p}^{n-1}(\theta)}{\tau^2} \right. \\ & \quad \left. - (1 - c_g^2) \frac{2(\cos(\beta - \theta h) - 1)}{h^2} \hat{p}^n(\theta) \right. \\ & \quad \left. + i\varepsilon c_g (\sin(\beta - \theta h) - \beta) \frac{e^{-i\alpha}\hat{p}^{n+1}(\theta) - e^{i\alpha}\hat{p}^{n-1}(\theta)}{\tau h} \right) d\theta = 0. \end{aligned}$$

We then have

$$\begin{aligned} & \varepsilon^2 \frac{e^{-i\alpha}(1+i\alpha)\hat{p}^{n+1}(\theta) - 2\hat{p}^n(\theta) + e^{i\alpha}(1-i\alpha)\hat{p}^{n-1}(\theta)}{\tau^2} \\ & - (1 - c_g^2) \frac{2(\cos(\beta - \theta h) - 1)}{h^2} \hat{p}^n(\theta) \\ & + i\varepsilon c_g (\sin(\beta - \theta h) - \beta) \frac{e^{-i\alpha}\hat{p}^{n+1}(\theta) - e^{i\alpha}\hat{p}^{n-1}(\theta)}{\tau h} = 0, \end{aligned}$$

which is equivalent to the system

$$\begin{pmatrix} \hat{p}^{n+1}(\theta) \\ \hat{p}^n(\theta) \end{pmatrix} = G(\theta) \begin{pmatrix} \hat{p}^n(\theta) \\ \hat{p}^{n-1}(\theta) \end{pmatrix},$$

where

$$G(\theta) = \begin{pmatrix} \frac{2\tilde{\gamma}_\theta e^{i\alpha}}{1+i\gamma_\theta} & -\frac{(1-i\gamma_\theta)e^{2i\alpha}}{1+i\gamma_\theta} \\ 1 & 0 \end{pmatrix} \quad (6.2)$$

with

$$\begin{aligned} \gamma_\theta &= \alpha + \frac{c_g \tau}{\varepsilon h} (\sin(\beta - \theta h) - \beta) = \alpha + \frac{\kappa c_g}{\kappa c_g - \omega} \frac{\alpha}{\beta} (\sin(\beta - \theta h) - \beta) \\ &= \alpha + \kappa^2 (1 - \sin(\beta - \theta h)/\beta) \alpha \\ \tilde{\gamma}_\theta &= 1 - (1 - c_g^2) \frac{\tau^2}{\varepsilon^2 h^2} (\cos(\beta - \theta h) - 1) \\ &= 1 + \frac{\kappa^2 (1 - c_g^2)}{\vartheta^2} \frac{\alpha^2}{\beta^2} (\cos(\beta - \theta h) - 1) \\ &= 1 - \kappa^2 \frac{\alpha^2}{\beta^2} (1 - \cos(\beta - \theta h)). \end{aligned}$$

To simplify the expressions of γ_θ and $\tilde{\gamma}_\theta$, we have used that $\kappa c_g/\vartheta = -\kappa^2 (1 - c_g^2)/\vartheta^2 = -\kappa^2$.

Let $\lambda_\theta^+, \lambda_\theta^-$ be the two roots of the characteristic polynomial

$$\rho_\theta(\zeta) = e^{-i\alpha} (1 + i\gamma_\theta) \zeta^2 - 2\tilde{\gamma}_\theta \zeta + e^{i\alpha} (1 - i\gamma_\theta),$$

i.e.,

$$\lambda_\theta^\pm = e^{i\alpha} \frac{\tilde{\gamma}_\theta \pm i\sqrt{(1 + |\gamma_\theta|^2) - |\tilde{\gamma}_\theta|^2}}{(1 + i\gamma_\theta)}.$$

Condition (3.4) ensures that $|\tilde{\gamma}_\theta| < \max\{1, |\gamma_\theta|\}$, and thus $|\lambda_\theta^\pm| = 1$. The vectors $(\lambda_\theta^+, 1)^\top$ and $(\lambda_\theta^-, 1)^\top$ are eigenvectors of $G(\theta)$ with eigenvalue λ_θ^+ and λ_θ^- , respectively. This is because (similar for λ_θ^-)

$$\begin{pmatrix} \frac{2c_2 e^{i\alpha}}{1+i\gamma_\theta} & -\frac{(1-i\gamma_\theta)e^{2i\alpha}}{1+i\gamma_\theta} \\ 1 & 0 \end{pmatrix} \begin{pmatrix} \lambda_\theta^+ \\ 1 \end{pmatrix} = \begin{pmatrix} \frac{(2c_2 e^{i\alpha} \lambda_\theta^+ - (1-i\gamma_\theta)e^{2i\alpha}}{1+i\gamma_\theta} \\ \lambda_\theta^+ \end{pmatrix} = \lambda_\theta^+ \begin{pmatrix} \lambda_\theta^+ \\ 1 \end{pmatrix}.$$

Therefore $G(\theta)$ is diagonalizable,

$$V(\theta)^{-1} G(\theta) V(\theta) = \Lambda(\theta) = \text{diag}\{\lambda_\theta^+, \lambda_\theta^-\} \quad \text{with} \quad V(\theta) = \begin{pmatrix} \lambda_\theta^+ & \lambda_\theta^- \\ 1 & 1 \end{pmatrix} \quad (6.3)$$

and $\Lambda(\theta)$ is a unitary matrix. Using the transformation matrix $V(\theta)$, we have, for any vector $y \in \mathbb{C}^2$,

$$|V(\theta)^{-1} G(\theta) y|_2 = |\Lambda(\theta) V(\theta)^{-1} y|_2 = |V(\theta)^{-1} y|_2.$$

Therefore,

$$\begin{aligned} \|\|P^n\|\| &:= \int_{\mathbb{R}} \left| V(\theta)^{-1} \begin{pmatrix} \hat{p}^{n+1}(\theta) \\ \hat{p}^n(\theta) \end{pmatrix} \right|_2 d\theta = \int_{\mathbb{R}} \left| V(\theta)^{-1} G(\theta) \begin{pmatrix} \hat{p}^n(\theta) \\ \hat{p}^{n-1}(\theta) \end{pmatrix} \right|_2 d\theta \\ &= \int_{\mathbb{R}} \left| V(\theta)^{-1} \begin{pmatrix} \hat{p}^n(\theta) \\ \hat{p}^{n-1}(\theta) \end{pmatrix} \right|_2 d\theta = \|\|P^{n-1}\|\|. \end{aligned}$$

Finally, we show that

$$\|V(\theta)\|_2 \leq C_1, \quad \|V(\theta)^{-1}\|_2 \leq C_2, \quad \forall \theta \in \mathbb{R},$$

which yields that the newly introduced norm $\|\cdot\|\|$ is equivalent to $\|\cdot\|_{A(\mathbb{R}) \times A(\mathbb{R})}$. Since

$$V(\theta)^* V(\theta) = \begin{pmatrix} \frac{2}{1 + \lambda_\theta^- \lambda_\theta^+} & 1 + \overline{\lambda_\theta^+} \lambda_\theta^- \\ 1 + \lambda_\theta^- \lambda_\theta^+ & \frac{2}{2} \end{pmatrix},$$

the eigenvalues of $V(\theta)^* V(\theta)$ can be calculated as $2 \left(1 \pm \sqrt{\frac{\tilde{\gamma}_\theta^2}{(1 + \gamma_\theta^2)}} \right)$. Since $\frac{\tilde{\gamma}_\theta^2}{(1 + \gamma_\theta^2)} \leq \mu < 1$ by condition (3.4), we have for all k that

$$\begin{aligned} \|V(\theta)\|_2 &= \sqrt{\lambda_{\max}(V(\theta)^* V(\theta))} < 2, \\ \|V(\theta)^{-1}\|_2 &= 1/\sqrt{\lambda_{\min}(V(\theta)^* V(\theta))} \leq 1/\sqrt{2(1 - \mu)}, \end{aligned}$$

so that

$$\frac{1}{2} \|P\|_{A(\mathbb{R}) \times A(\mathbb{R})} \leq \|\|P\|\| \leq \frac{1}{\sqrt{2(1 - \mu)}} \|P\|_{A(\mathbb{R}) \times A(\mathbb{R})}$$

for all $P \in A(\mathbb{R}) \times A(\mathbb{R})$. \square

Lemma 6.2 (Linear stability of the weighted Crank–Nicolson method)
The weighted Crank–Nicolson algorithm (3.6) without the nonlinear term is unconditionally stable in the sense that there exists a norm $\|\cdot\|\|$ on $A(\mathbb{R}) \times A(\mathbb{R})$, equivalent to the norm $\|\cdot\|_{A(\mathbb{R}) \times A(\mathbb{R})}$ uniformly in ε, τ, h , such that

$$\|\|P^n\|\| = \|\|P^{n-1}\|\|, \quad \text{where } P^n = \begin{pmatrix} p^{n+1} \\ p^n \end{pmatrix}.$$

Proof Substituting the Fourier transform of p^n into (3.6) without the nonlinear term yields

$$\begin{aligned} &\varepsilon^2 \frac{e^{-i\alpha}(1 + i\alpha)\hat{p}^{n+1}(\theta) - 2\hat{p}^n(\theta) + e^{i\alpha}(1 - i\alpha)\hat{p}^{n-1}(\theta)}{\tau^2} \\ &- (1 - c_g^2) \frac{2(\cos(\beta - \theta h) - 1)}{h^2} \frac{e^{-i\alpha}\hat{p}^{n+1}(\theta) + e^{i\alpha}\hat{p}^{n-1}(\theta)}{2} \\ &+ i\varepsilon c_g (\sin(\beta - \theta h) - \beta) \frac{e^{-i\alpha}\hat{p}^{n+1}(\theta) - e^{i\alpha}\hat{p}^{n-1}(\theta)}{\tau h} = 0, \end{aligned}$$

which is equivalent to the system

$$\begin{pmatrix} \hat{p}^{n+1}(\theta) \\ \hat{p}^n(\theta) \end{pmatrix} = G(\theta) \begin{pmatrix} \hat{p}^n(\theta) \\ \hat{p}^{n-1}(\theta) \end{pmatrix},$$

where

$$G(\theta) = \begin{pmatrix} \frac{2e^{i\alpha}}{\gamma_\theta} & -\frac{\overline{\gamma_\theta}e^{2i\alpha}}{\gamma_\theta} \\ 1 & 0 \end{pmatrix},$$

with $\gamma_\theta = 1 + \frac{(1-c_g^2)\tau^2}{\varepsilon^2 h^2} (1 - \cos(\beta - \theta h)) + i\alpha + i\frac{c_g\tau}{\varepsilon h} (\sin(\beta - \theta h) - \beta)$. Since $|\gamma_\theta|^2 > 1$, the eigenvalues of $G(\theta)$ are

$$\lambda_\theta^\pm = \frac{e^{i\alpha}}{\gamma_\theta} \left(1 \pm i\sqrt{|\gamma_\theta|^2 - 1} \right)$$

and $|\lambda_\theta^\pm| = 1$ for all θ . Following the same procedure as in the proof of Lemma 6.3 yields the desired result. \square

6.2 Nonlinear stability

Lemma 6.3 (Nonlinear stability of the weighted leapfrog method)
Let the function $\tilde{p} \in C([0, T], A(\mathbb{R}))$ be arbitrary and let the corresponding defect d be defined by (5.1). Under condition (3.4), the interpolated numerical solution of (3.1), interpolated to all $\xi \in \mathbb{R}$ as in (6.1) (but now with the nonlinear term included), satisfies the bound, for $t_n = n\tau \leq T$

$$\begin{aligned} & \|p^n - \tilde{p}(t_n, \cdot)\|_{A(\mathbb{R})} \\ & \leq C \left(\|p^0 - \tilde{p}(0, \cdot)\|_{A(\mathbb{R})} + \|p^1 - \tilde{p}(t_1, \cdot)\|_{A(\mathbb{R})} + \|d\|_{C([0, T], A(\mathbb{R}))} \right), \end{aligned}$$

where C is independent of ε , τ , h , and n with $t_n \leq T$, but depends on T and on upper bounds of the above term in big brackets and of the $C([0, T], A(\mathbb{R}))$ norm of p .

Proof We define the error function $e^n(\xi) = p^n(\xi) - \tilde{p}(t_n, \xi)$, which satisfies

$$\begin{aligned} & \varepsilon^2 \frac{e^{-i\alpha}(1 + i\alpha)e^{n+1}(\xi) - 2e^n(\xi) + e^{i\alpha}(1 - i\alpha)e^{n-1}(\xi)}{\tau^2} \\ & + (c_g^2 - 1) \frac{e^{-i\beta}e^n(\xi + h) - 2e^n(\xi) + e^{i\beta}e^n(\xi - h)}{h^2} \\ & - 2\varepsilon c_g \left(\frac{e^{-i\alpha}(e^{-i\beta}e^{n+1}(\xi + h) - e^{i\beta}e^{n+1}(\xi - h))}{4\tau h} \right. \\ & \quad \left. - \frac{e^{i\alpha}(e^{-i\beta}e^{n-1}(\xi + h) - e^{i\beta}e^{n-1}(\xi - h))}{4\tau h} \right. \\ & \quad \left. + \frac{i\beta(e^{-i\alpha}e^{n+1}(\xi) - e^{i\alpha}e^{n-1}(\xi))}{2\tau h} \right) \\ & + \lambda (|p^n(\xi)|^2 p^n(\xi) - |\tilde{p}(t_n, \xi)|^2 \tilde{p}(t_n, \xi)) \\ & = -d(t, \xi). \end{aligned} \tag{6.4}$$

The Fourier transform of e^n then satisfies

$$\begin{aligned} & \varepsilon^2 \frac{e^{-i\alpha}(1+i\alpha)\hat{e}^{n+1}(\theta) - 2\hat{e}^n(\theta) + e^{i\alpha}(1-i\alpha)\hat{e}^{n-1}(\theta)}{\tau^2} \\ & + - (1 - c_g^2) \frac{2(\cos(\theta h) - 1)}{h^2} \hat{e}^n(\theta) \\ & + i\epsilon c_g (\sin(\beta - \theta h) - \beta) \frac{e^{-i\alpha}\hat{e}^{n+1}(\theta) - e^{i\alpha}\hat{e}^{n-1}(\theta)}{\tau h} + \hat{d}^n(\theta) \\ & + \lambda \mathcal{F}(|p^n(\xi)|^2 p^n(\xi) - |\tilde{p}(t_n, \xi)|^2 \tilde{p}(t_n, \xi)) = 0, \end{aligned}$$

This equation can be written in the one-step formulation

$$\begin{pmatrix} \hat{e}^{n+1}(\theta) \\ \hat{e}^n(\theta) \end{pmatrix} = G(\theta) \begin{pmatrix} \hat{e}^n(\theta) \\ \hat{e}^{n-1}(\theta) \end{pmatrix} - \frac{\tau^2}{\varepsilon^2(1+i\gamma_\theta)} \begin{pmatrix} \hat{d}^n(\theta) \\ 0 \end{pmatrix} - \lambda \frac{\tau^2}{\varepsilon^2(1+i\gamma_\theta)} \begin{pmatrix} \mathcal{F}(|p^n(\xi)|^2 p^n(\xi) - |\tilde{p}(t_n, \xi)|^2 \tilde{p}(t_n, \xi))(\theta) \\ 0 \end{pmatrix}$$

with γ_θ and $G(\theta)$ defined in (6.2). Note that $\left| \frac{\tau^2}{\varepsilon^2(1+i\gamma_\theta)} \right| \sim \tau$. Introducing $\mathcal{E}^n = \begin{pmatrix} e^{n+1} \\ e^n \end{pmatrix}$, using Lemma 6.1 and (2.3) for dealing with the nonlinearity, we obtain

$$\begin{aligned} \|\mathcal{E}^n\| & \leq (1 + c\tau) \|\mathcal{E}^{n-1}\| + \tilde{c}\tau \|d(t_n, \cdot)\|_{A(\mathbb{R})} \\ & \leq (1 + c\tau)^n \|\mathcal{E}^0\| + \tilde{c}\tau \sum_{j=1}^n (1 + c\tau)^{n-j} \|d(t_j, \cdot)\|_{A(\mathbb{R})} \\ & \leq \exp(cn\tau) \|\mathcal{E}^0\| + \tilde{c}\tau \frac{\exp(cn\tau) - 1}{c\tau} \sup_{t \in [0, T]} \|d(t, \cdot)\|_{A(\mathbb{R})}, \end{aligned}$$

which yields the result. \square

The same nonlinear stability bound (possibly with a different constant C) is obtained for the weighted Crank–Nicolson method without any CFL-type condition between τ and h and ε , using the same arguments together with Lemma 6.2.

With Lemmas 5.2 and 6.3 at hand, we are finally in the position to prove Theorems 4.1–4.3.

Proof of Theorems 4.1 and 4.2. Combined with Lemma 5.2 (consistency), Lemma 6.3 (stability) establishes the dominant terms in the modulated Fourier expansion of the numerical solution as stated in Theorem 4.1. Comparing this expansion with the modulated Fourier expansion of the exact solution in Proposition 2.1 then yields the solution error bound stated in Theorem 4.2.

The proof of Proposition 2.1 gives the velocity

$$\varepsilon^2 \partial_t u(t, x) = -i\omega a^+(t, \xi) e^{i(\kappa x - \omega t/\varepsilon)/\varepsilon} + i\omega a^-(t, \eta) e^{i(\kappa x + \omega t/\varepsilon)/\varepsilon} + \mathcal{O}(\varepsilon),$$

which, together with Theorem 4.1, leads to the velocity error estimate in Theorem 4.2. \square

Proof of Theorem 4.3. The higher-order accuracy in ε for the solution u follows from the polarized approximation in Proposition 2.2 together with the refined defect estimate for the numerical solution given in Remark 5.1.

For the velocity approximation, Proposition 2.2 gives

$$\varepsilon^2 \partial_t \tilde{u}(t, x) = -(\mathrm{i}\omega(a(t, \xi) + \varepsilon b(t, \xi)) + \varepsilon c_g \partial_\xi a(t, \xi)) e^{\mathrm{i}(\kappa x - \omega t/\varepsilon)/\varepsilon} + \mathcal{O}(\varepsilon^2).$$

Comparing this expression with (3.5) then yields the second error bound. \square

Acknowledgement

This work was supported by the Deutsche Forschungsgemeinschaft (DFG, German Research Foundation) – Project-ID258734477 – SFB 1173.

References

1. W. Bao, Y. Cai, and X. Zhao. A uniformly accurate multiscale time integrator pseudospectral method for the Klein–Gordon equation in the nonrelativistic limit regime. *SIAM Journal on Numerical Analysis*, 52(5):2488–2511, 2014.
2. W. Bao and X. Dong. Analysis and comparison of numerical methods for the Klein–Gordon equation in the nonrelativistic limit regime. *Numerische Mathematik*, 120(2):189–229, 2012.
3. W. Bao and X. Zhao. Comparison of numerical methods for the nonlinear Klein–Gordon equation in the nonrelativistic limit regime. *Journal of Computational Physics*, 398:108886, 2019.
4. J. Baumstark, T. Jahnke, and C. Lubich. Polarized high-frequency wave propagation beyond the nonlinear Schrödinger approximation. *SIAM Journal on Mathematical Analysis*, 56(1):454–473, 2024.
5. S. Baumstark, E. Faou, and K. Schratz. Uniformly accurate exponential-type integrators for Klein–Gordon equations with asymptotic convergence to the classical NLS splitting. *Mathematics of Computation*, 87(311):1227–1254, 2018.
6. P. Chartier, N. Crouseilles, M. Lemou, and F. Méhats. Uniformly accurate numerical schemes for highly oscillatory Klein–Gordon and nonlinear Schrödinger equations. *Numerische Mathematik*, 129:211–250, 2015.
7. M. Colin and D. Lannes. Short pulses approximations in dispersive media. *SIAM Journal on Mathematical Analysis*, 41(2):708–732, 2009.
8. N. Crouseilles, S. Jin, and M. Lemou. Nonlinear geometric optics method-based multiscale numerical schemes for a class of highly oscillatory transport equations. *Mathematical Models and Methods in Applied Sciences*, 27(11):2031–2070, 2017.
9. X. Dong, Z. Xu, and X. Zhao. On time-splitting pseudospectral discretization for nonlinear Klein–Gordon equation in nonrelativistic limit regime. *Communications in Computational Physics*, 16(2):440–466, 2014.
10. E. Faou and K. Schratz. Asymptotic preserving schemes for the Klein–Gordon equation in the non-relativistic limit regime. *Numerische Mathematik*, 126(3):441–469, 2014.
11. T. Jahnke and J. Mödl. Analytical and numerical approximations to highly oscillatory solutions of nonlinear Friedrichs systems. *CRC 1173 Preprint 2024/22, KIT*, 2024.
12. Y. Katznelson. *An introduction to harmonic analysis*. Dover Publications, Inc., New York, corrected edition, 1976.
13. P. Kirrman, G. Schneider, and A. Mielke. The validity of modulation equations for extended systems with cubic nonlinearities. *Proceedings of the Royal Society of Edinburgh: Section A Mathematics*, 122(1–2):85–91, 1992.
14. R. D. Pierce and C. E. Wayne. On the validity of mean-field amplitude equations for counterpropagating wavetrains. *Nonlinearity*, 8(5):769, 1995.
15. Y. Shi and C. Lubich. Weighted finite difference methods for the semiclassical nonlinear Schrödinger equation with multiphase oscillatory initial data. *arXiv preprint arXiv:2508.15683*, 2025.